



**HAL**  
open science

# Extending the scope and understanding of all-optical magnetization switching in Gd-based alloys by controlling the underlying temperature transients

Maxime Verges, Wei Zhang, Quentin Remy, Yann Le Guen, Jon Gorchon, Grégory Malinowski, Stephane Mangin, Michel Hehn, Julius Hohlfeld

## ► To cite this version:

Maxime Verges, Wei Zhang, Quentin Remy, Yann Le Guen, Jon Gorchon, et al.. Extending the scope and understanding of all-optical magnetization switching in Gd-based alloys by controlling the underlying temperature transients. *Physical Review Applied*, 2024, 21 (4), pp.044003. 10.1103/physrevapplied.21.044003 . hal-04585716

**HAL Id: hal-04585716**

**<https://hal.science/hal-04585716v1>**

Submitted on 23 May 2024

**HAL** is a multi-disciplinary open access archive for the deposit and dissemination of scientific research documents, whether they are published or not. The documents may come from teaching and research institutions in France or abroad, or from public or private research centers.

L'archive ouverte pluridisciplinaire **HAL**, est destinée au dépôt et à la diffusion de documents scientifiques de niveau recherche, publiés ou non, émanant des établissements d'enseignement et de recherche français ou étrangers, des laboratoires publics ou privés.

# Extending the scope and understanding of all-optical magnetization switching in Gd-based alloys by controlling the underlying temperature transients

Maxime Verges<sup>1</sup>, Wei Zhang, Quentin Remy, Yann Le-Guen, Jon Gorchon<sup>1</sup>, Gregory Malinowski, Stephane Mangin<sup>1</sup>,\* Michel Hehn, and Julius Hohlfeld<sup>1</sup>

*Institut Jean Lamour, CNRS UMR 7198, Université de Lorraine, Vandoeuvre-lès-Nancy F-54506, France*



(Received 22 September 2023; revised 7 February 2024; accepted 27 February 2024; published 1 April 2024)

We use the thickness of Cu layers to control all-optical switching of magnetization in adjacent  $\text{Gd}_{24}(\text{Fe}_{90}\text{Co}_{10})_{76}$  films. While increasing the Cu thickness from 5 to 900 nm has no effect on the switching threshold, it significantly enlarges the fluence and pulse duration at which multiple domains emerge. Having shown that thermally activated multidomain formation limits the maximum fluence and pulse duration for controlled switching, we demonstrate that continuous magnetization reversal precedes multidomain formation in  $\text{Gd}_{18}\text{Dy}_4\text{Co}_{78}$  films excited with fluences slightly larger than the multidomain threshold.

DOI: [10.1103/PhysRevApplied.21.044003](https://doi.org/10.1103/PhysRevApplied.21.044003)

## I. INTRODUCTION

Optical excitation of ferrimagnetic rare earth and transition metal (RE-TM) alloys and multilayers by a single, arbitrary polarized laser pulse can lead to ultrafast magnetization reversal when the fluence and duration of this pulse stay within mutually dependent bounds [1–8]. In Gd-based samples, this so-called all-optical helicity independent switching (AOHIS) [also known as temperature-induced magnetization switching (TIMS)] results from transient spin transfer between the two magnetic subsystems by angular momentum conserving exchange scattering that originates from their different de- and remagnetization rates in response to laser-pulse-induced changes of the electron temperature. This understanding is the essence of so many experimental and theoretical investigations that it is impossible to do justice to each single one of them. Four experiments, showing the appearance of a transient ferromagnetic state during the reversal [6] and magnetization reversal due to picosecond heat pulses resulting from current-pulse-induced joule heating [9] and from fast heat diffusion through thick gold films [10,11], stand out as key demonstrations of the exchange- and temperature-driven nature of the magnetization reversal in Gd-Fe-Co, respectively.

Theoretical works have identified the dominance of spin transfer between the magnetic subsystems over spin transfer to the lattice as a prerequisite for AOHIS [12–22], derived preconditions for the magnetization magnitudes of both subsystems from this switching criterion [23], and qualitatively reproduced the impact of Gd concentration, laser fluence, and initial temperature on AOHIS

[15,24]. However, the questions if the fluence thresholds for the appearance of controlled AOHIS and of stochastic multidomain formation are linked to thresholds for the maximum electron temperature [25] or not [1,8] and if the maximum pulse duration leading to AOHIS is limited by a breakdown of the underlying switching mechanism [2], or by thermal erasure at longer time delays [3] are still a matter of debate.

In this paper, we use the thickness of Cu heat sinks,  $t_{\text{Cu}}$ , to control the transient laser-pulse-induced increase of the electron temperature within adjacent 10-nm-thick Gd-Fe-Co films,  $\Delta T_e(t)$ , that results from their excitation by short laser pulses of various fluence,  $F_{\text{las}}$ , and pulse duration,  $\tau_{\text{las}}$ . This allows us to use slight adjustments of the laser fluence as means to tailor  $\Delta T_e(t)$  for any given laser-pulse duration, such that identical heating dynamics are followed by faster and stronger cooling for thicker heat sinks (cf. Fig. 1). In this way we are able to disentangle the impact of  $\Delta T_e$  at short times, where it reaches its maximum, and at longer times, where it is in quasiequilibrium with the elevated phonon temperature, on the fluence thresholds for controlled switching,  $F_{\text{sw}}$ , and of stochastic multidomain formation,  $F_{\text{MD}}$ . We derive both thresholds from domain images acquired via static linear magneto-optical microscopy.

## II. MODELING

Throughout this paper, we use numerical solutions of the two-temperature model (TTM) to qualitatively explain the impact of Cu heat sinks on the temperature dynamics in Gd-Fe-Co. The quantitative significance of those solutions is limited by the shortcomings of the TTM itself (the basic assumption of well-defined electron and phonon temperatures at all times is definitely invalid at short time

\*Corresponding author. [stephane.mangin@univ-lorraine.fr](mailto:stephane.mangin@univ-lorraine.fr)

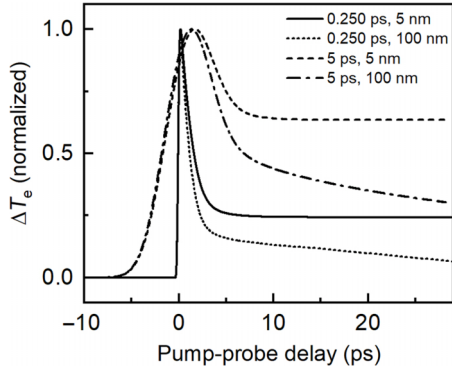


FIG. 1. Transients of  $\Delta T_e / \Delta T_{e,\max}$  within Gd-Fe-Co predicted by the TTM for  $\tau_{\text{las}}$  and  $t_{\text{Cu}}$  given in the legend. In our experiments, typical values of  $\Delta T_{e,\max}$  range from approximately equal to 300 K for long pulses and small fluences up to approximately equal to 2000 K for short pulses and high fluences.

delays) as well as by the uncertainty of the used material parameters. Since the TTM results are only used to set qualitative expectations, we refrain from an in-depth discussion of our model. We want only to mention that the calculations are performed for the whole sample stack with the common assumptions of negligible lateral temperature gradients and zero interface resistance for phonons. The boundary condition of equal electron temperatures at the interface between adjacent metallic layers leads to maximum electron temperatures in Cu that are predominantly governed by the large electronic heat capacity of Gd-Fe-Co, which is in line with earlier investigations of transient temperature dynamics in Ni/Au bilayers [26].

### III. STATIC MEASUREMENTS

The investigated samples are grown by dc magnetron sputtering onto glass substrates in the following multilayered structure: glass/Ta(3)/Cu(5)/Gd<sub>24</sub>(Fe<sub>90</sub>Co<sub>10</sub>)(10)/Cu( $t_{\text{Cu}}$ )/Pt(5), where the numbers in brackets give the layer thickness in nm. The bottom Ta and Cu layers improve adhesion of the structure to the glass substrate and ensure that the Gd-Fe-Co layer exhibits perpendicular magnetic anisotropy, respectively [27]. They are thin enough to effectively pump the Gd-Fe-Co layer and probe its magnetic state via measurements of the linear magneto-optical Kerr effect from the substrate side. The Pt-capping layer prevents oxidation of the sample. The thickness of the upper Cu heat sink wedges,  $t_{\text{Cu}}$ , varies linearly across the 2.5-cm-wide samples over the following ranges (in nm): [5,10], [10,15], [10,20], [20,30], [35,70], [70,105], [50,100], [100,150], [100,200], [200,300], [300,600], and [600,900]. Great care was taken to ensure identical compositions and magnetic properties of all Gd-Fe-Co layers, which was confirmed by the demonstration of identical hysteresis loops and equal fluence thresholds for different samples with equal  $t_{\text{Cu}}$  as shown in Fig. 2.

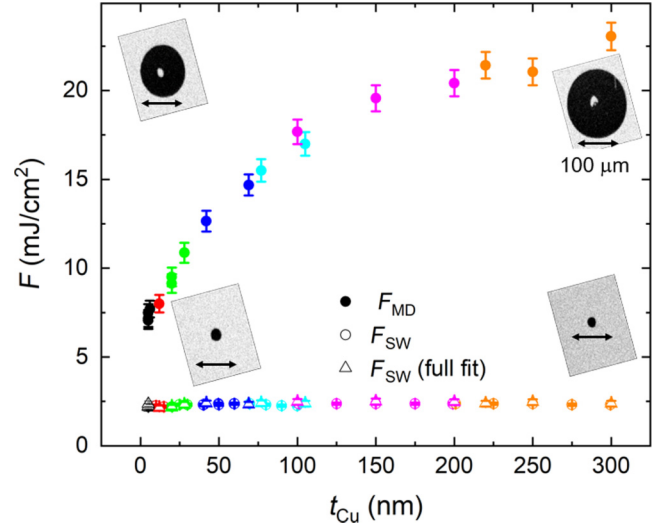


FIG. 2.  $F_{\text{SW}}$  and  $F_{\text{MD}}$  versus the heat-sink thickness,  $t_{\text{Cu}}$ , for different samples (distinguished by the symbol color) and  $s$ -polarized, 750-nm laser pulses of 150-fs duration incident at approximately equal to  $5^\circ$ . Open triangles represent results of the fits used to determine the beam size. Insets show typical domains written at  $F_{\text{SW}}$  and  $F_{\text{MD}}$  for  $t_{\text{Cu}} = 5$  and 300 nm, respectively.

The fluence thresholds  $F_{\text{SW}}$  and  $F_{\text{MD}}$  are derived from the size and quality of written domains imaged as function of  $F_{\text{las}}$ ,  $\tau_{\text{las}}$ , and  $t_{\text{Cu}}$  by magneto-optical microscopy (cf. insets of Fig. 2). We first calibrate this derivation by simultaneously fitting the radii  $r_{x/y}$  of the switched domains observed in samples with particular heat-sink thicknesses after their excitation by  $p$ -polarized, 800-nm, 150-fs laser pulses of various pulse energies,  $E_{\text{las}}$ , to

$$r_{x/y} = \sigma_{x/y} \sqrt{\ln \left( \frac{E_{\text{las}}}{\pi \sigma_x \sigma_y F_{\text{SW}}} \right)}, \quad (1)$$

where  $x$  and  $y$  are orthogonal axis defining the sample plane and  $\sigma_{x/y}$  denote the corresponding widths of our slightly elliptical, Gaussian laser beam on the sample. The laser-spot area obtained from these fits is then used to convert the measured pulse-energy thresholds for the appearance of reversed domains at other values of  $t_{\text{Cu}}$ , and of nonreversed domains within the written ones into  $F_{\text{SW}}$  and  $F_{\text{MD}}$ , respectively.

The corresponding results, obtained on various samples with partially overlapping Cu thicknesses are shown in Fig. 2 for  $t_{\text{Cu}} \in [5, 300]$  nm. They reveal that  $F_{\text{SW}}$  is independent of  $t_{\text{Cu}}$ , but that  $F_{\text{MD}}$  strongly increases with  $t_{\text{Cu}}$  in a way that resembles the increase of femtosecond laser-pulse damage thresholds of gold films with their thickness [28]. In analogy to the fact that the damage threshold of Au is governed by  $T_{e,\text{eq}} = T_{\text{melt}}$ , with  $T_{e,\text{eq}}$  and  $T_{\text{melt}}$  denoting the electron temperature at the time when

they reach thermal equilibrium with the phonons and the melting point, respectively, this resemblance indicates that multidomain formation is also governed by a threshold condition for  $T_e$  at longer time delays.

We repeated the procedure outlined above to determine the impact of the laser-pulse duration on  $F_{\text{SW}}$  and  $F_{\text{MD}}$  for selected heat-sink thicknesses shown in Fig. 3. Throughout the investigated pulse duration range from 250 fs to 10 ps, we find that the values of  $F_{\text{SW}}$  monotonously increase with  $\tau_{\text{las}}$  but are independent of  $t_{\text{Cu}}$  [cf. panels (a) and (c)]. A comparison of these findings to TTM calculations with typical material parameters as published in Refs. [1,29,30] shows, that both results contradict the hypothesis of a  $T_{e,\text{max}}$ -defined switching criterion for AOHIS. In order to induce identical values of  $T_{e,\text{max}}$  in samples with  $t_{\text{Cu}} = 5$  nm, the fluence of 5-ps pulses would have to be about 4 times larger than the one of 250-fs pulses—about twice as large as the measured ratio. Moreover, in order to compensate for cooling of the electrons due to heat diffusion into the heat sink during the excitation,  $F_{\text{SW}}$  would have to increase with  $t_{\text{Cu}}$  if the appearance of switching would be related to  $T_{e,\text{max}}$ . According to the TTM, about 40% larger fluences are needed to reach the same  $T_{e,\text{max}}$  with 5-ps pulses in samples with  $t_{\text{Cu}} = 200$  nm as in those with  $t_{\text{Cu}} = 5$  nm. In line with the work of Gorchon *et al.* [1], the incompatibility of our data and TTM calculations suggests that  $F_{\text{SW}}$  is not directly related to  $T_{e,\text{max}}$ . Note, that we deliberately state this is not proven since

the quantitative significance of our TTM predictions is limited.

Now we draw our attention to the impact of  $t_{\text{Cu}}$  and  $\tau_{\text{las}}$  on  $F_{\text{MD}}$ . As shown in Fig. 3(b), we find that  $F_{\text{MD}}$  increases with  $t_{\text{Cu}}$  in a way that resembles exponential saturation functions,  $F_{\text{MD}} = F_0 + \Delta F \cdot (1 - \exp(-t_{\text{Cu}}/\lambda_{\text{Cu}}))$  with characteristic amplitudes,  $\Delta F$ , and lengths,  $\lambda_{\text{Cu}}$ , that decrease and increase with  $\tau_{\text{las}}$ , respectively. The behavior of  $\Delta F$  is qualitatively reproduced by our TTM calculations and reflects the changing character of heat diffusion with increasing pulse duration. While short pulses lead to thermal diffusion by hot electrons that rapidly spreads the absorbed energy over a range of  $\lambda_{\text{th,e}} \approx 230$  nm before electrons and phonons reach thermal equilibrium, long pulses are followed by much slower phonon-dominated diffusion that spreads the energy only over  $\lambda_{\text{th,ph}} \approx 60$  nm within 10 ps [28,31]. In contrast, the increase of  $\lambda_{\text{Cu}}$  with  $\tau_{\text{las}}$  (related to the slight uptick of  $F_{\text{MD}}$  with  $t_{\text{Cu}} \in [300, 900]$  nm observed for long pulse durations) cannot be explained in terms of temperature dynamics alone and might be caused by magnetic contributions to the formation of multiple domains [32,33].

The demonstration of a strong increase of the multidomain threshold with the heat-sink thickness constitutes the most useful result of this work. It proves, independent of any model, that values of  $F_{\text{MD}}$  reported for non-heat-sunk samples do not reflect a breakdown of the material-specific reversal mechanism due to an exceedingly high maximum

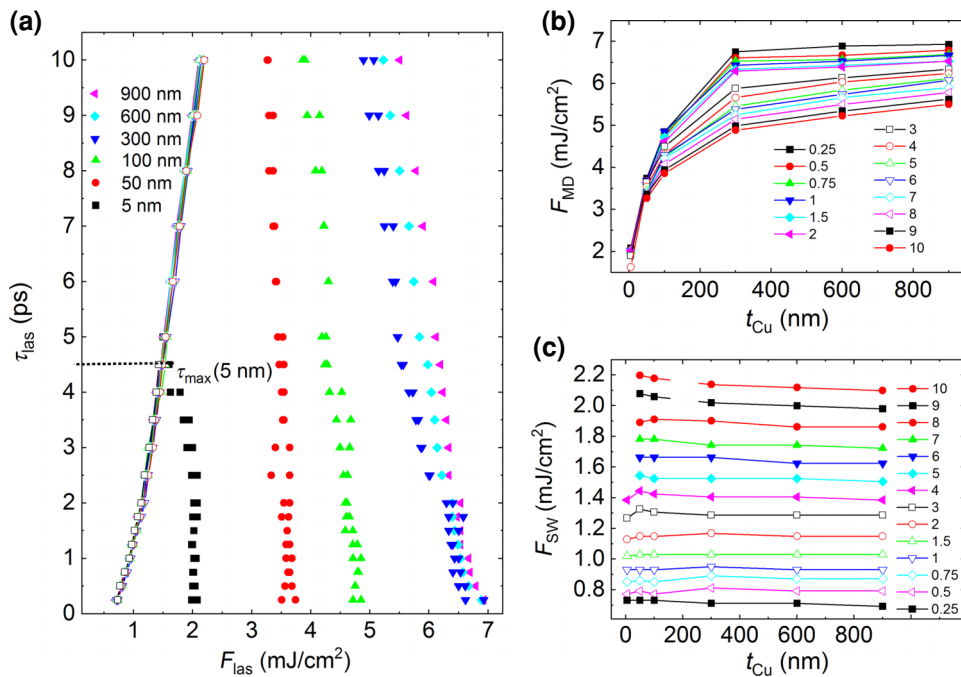


FIG. 3. (a)  $F_{\text{SW}}(\tau_{\text{las}})$  (open symbols and lines) and  $F_{\text{MD}}(\tau_{\text{las}})$  (closed symbols) for different  $t_{\text{Cu}}$  given in the legend. The dashed line indicates  $\tau_{\text{max}}(t_{\text{Cu}} = 5 \text{ nm})$ . (b)  $F_{\text{MD}}$  versus  $t_{\text{Cu}}$  for various  $\tau_{\text{las}}$  given in the legend in ps. (c) Same as (b) but for  $F_{\text{SW}}$ . All data are for  $p$ -polarized, 800-nm pulses incident at approximately  $56^\circ$ .



electron temperature. Instead, the temperature of insufficiently cooled electrons becomes so large at  $F_{MD}$ , that it leads to complete demagnetization and/or activates dipolar field-driven multidomain formation at times longer than the electron-phonon equilibration time [32,33]. Moreover, it reveals that the maximum pulse duration applicable for controlled AOHIS,  $\tau_{max}$ , is not limited by accelerated demagnetization of Gd [2] but by thermally activated multidomain formation. As obvious from Fig. 3(a),  $\tau_{max}$  is defined by  $F_{SW}(\tau_{max}) = F_{MD}(\tau_{max})$ , so that an increase of  $F_{MD}$  with  $t_{Cu}$  enlarges  $\tau_{max}$ . The impact of  $F_{MD}(t_{Cu})$  on  $\tau_{max}$  is so strong, that  $\tau_{max}$  already exceeds our experimental pulse-length limit of 10 ps for  $t_{Cu} = 50$  nm. Linear data extrapolation suggests that pulses as long as 25 ps could be used for AOHIS in samples with  $t_{Cu} = 900$  nm.

#### IV. TIME-RESOLVED MEASUREMENTS

So far, we used static images of magnetization patterns resulting from the illumination of *multiple samples* (with distinct  $t_{Cu}$ ) by laser pulses of *various fluences* to prove that  $F_{MD}$  is not governed by a breakdown of the reversal mechanism of AOHIS. Now, we show that investigations of the spatiotemporal magnetization changes within a *single sample* induced by laser pulses of *one fixed fluence* might prove this fact as well. To provide such proof, the time-resolved images need to demonstrate that laser-pulse excitation with  $F_{las} \geq F_{MD}$  are followed by spatially continuous magnetization reversal before the magnetization breaks up into multiple domains. Consequently, the time-resolved approach works only for samples where large dipolar fields and/or small magnetocrystalline anisotropies lead to the formation of multidomains at temperatures so far below the Curie point, that the laser-heated electrons at no time cause complete demagnetization. This implies that the multidomain thresholds for femtosecond laser-pulse excitation of suitable samples do not exceed  $F_{SW}$  by much, if at all. Since this criterion is not fulfilled for the samples investigated so far (they exhibit  $F_{MD}/F_{SW} \geq 3$ ), we demonstrate the viability of the time-resolved approach by example of a glass/Ta(5)/Pt(3)/ $\alpha$ -Gd<sub>18</sub>Dy<sub>4</sub>Co<sub>78</sub>(10)/Pt(5) sample whose multidomain threshold is just approximately equal to 29% larger than  $F_{SW} = 4.6$  mJ/cm<sup>2</sup> for  $s$ -polarized 150-fs, 800-nm pulses incident at approximately equal to 5°.

Both, the fluence-dependent magnetization dynamics shown in Fig. 4(a), and the magnetization patterns measured at short and long delays given in Figs. 4(b) and 4(c), respectively, clearly attest that the excitation of this sample by 150-fs laser pulses with  $F_{las} = 1.12 \times F_{MD}$  is followed by ultrafast, continuous magnetization reversal before elevated electron temperatures in quasiequilibrium with the phonon temperature activate the dipolar field-driven formation of multiple domains.

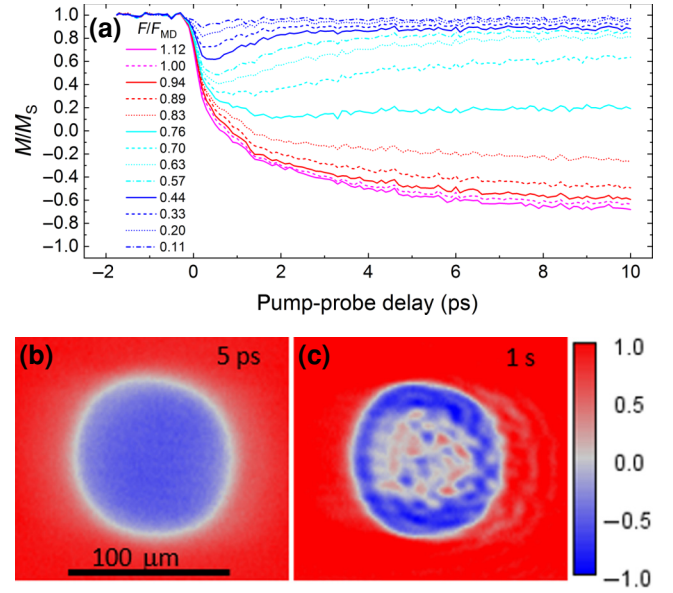


FIG. 4. (a) Magnetization dynamics in  $\alpha$ -Gd<sub>18</sub>Dy<sub>4</sub>Co<sub>78</sub> induced by  $s$ -polarized, 150-fs, 800-nm laser pulses of various fluences (given in multiples of  $F_{MD} = 5.9$  mJ/cm<sup>2</sup>) incident at approximately equal to 5°. Panels (b),(c) show normalized magnetization profiles 5 ps and 1 s after the excitation, respectively.

#### V. CONCLUSION

In conclusion we have used the thickness of Cu heat sinks to control the electron temperature dynamics following optical excitation of adjacent Gd-Fe-Co films by laser pulses of various duration and fluence. This enabled us to separately study the impact of the electron temperature at short times, where it reaches its maximum, and at longer times, where it is in quasiequilibrium with the phonon temperature, on the fluence thresholds for the onset of controlled temperature-induced switching and of stochastic multidomain formation. The measured variations of these thresholds with the heat-sink thickness and laser-pulse duration evidence that neither one is solely governed by  $T_{e,max}$ . We have shown that  $F_{MD}$  corresponds to the fluence where the temperature of insufficiently cooled electrons becomes so large that it causes complete demagnetization and/or activates dipolar field-driven multidomain formation at times longer than the electron-phonon equilibration time. Based on this insight we predict that excitation of samples whose multidomain threshold does not exceed the switching threshold by much, if at all, with laser fluences slightly larger than  $F_{MD}$  lead to controlled switching before the magnetization breaks up into multiple domains. We confirmed this prediction by example of Gd<sub>18</sub>Dy<sub>4</sub>Co<sub>78</sub>, with  $F_{MD}/F_{SW} \approx 1.29$  and  $F_{las} = 1.12 \times F_{MD}$ . Last, but not least, we have shown that any increase of  $F_{MD}$  with the heat-sink thickness lengthens the maximum pulse duration applicable for

AOHIS and derived an upper limit of  $\tau_{\max} \approx 25$  ps for  $\text{Gd}_{24}(\text{Fe}_{90}\text{Co}_{10})_{76}$  from linear extrapolation of our data. We expect that thermal management by metallic heat sinks will not only pave the way for future technological applications of AOHIS with laser pulses emitted by cheap laser diodes, but will also lead to the demonstration of AOHIS in many ferrimagnetic alloys and multilayers that were believed to show only multidomain formation as already demonstrated for  $\text{Gd}_{13}\text{Dy}_7\text{Co}_{80}$  in Ref. [34].

- 
- [1] J. Gorchon, R. B. Wilson, Y. Yang, A. Pattabi, J. Y. Chen, L. He, J. P. Wang, M. Li, and J. Bokor, Role of electron and phonon temperatures in the helicity-independent all-optical switching of GdFeCo, *Phys. Rev. B* **94**, 184406 (2016).
- [2] C. Davies, T. Janssen, J. Mentink, A. Tsukamoto, A. Kimel, A. van der Meer, A. Stupakiewicz, and A. Kirilyuk, Pathway for single-shot all-optical switching of magnetization in ferrimagnets, *Phys. Rev. Appl.* **13**, 024064 (2020).
- [3] J. Wei, B. Zhang, M. Hehn, W. Zhang, G. Malinowski, Y. Xu, W. Zhao, and S. Mangin, All-optical helicity-independent switching state diagram in Gd-Fe-Co alloys, *Phys. Rev. Appl.* **15**, 054065 (2021).
- [4] C. E. Graves, A. H. Reid, T. Wang, B. Wu, S. de Jong, K. Vahaplar, I. Radu, D. P. Bernstein, M. Messerschmidt, L. Müller *et al.*, Nanoscale spin reversal by non-local angular momentum transfer following ultrafast laser excitation in ferromagnetic GdFeCo, *Nat. Mater.* **12**, 293 (2013).
- [5] M. L. M. Lalieu, M. J. G. Peeters, S. R. R. Haenen, R. Lavrijsen, and B. Koopmans, Deterministic all-optical switching of synthetic ferrimagnets using single femtosecond laser pulses, *Phys. Rev. B* **96**, 220411 (2017).
- [6] I. Radu, K. Vahaplar, C. Stamm, T. Kachel, N. Pontius, H. A. Dürr, T. A. Ostler, J. Barker, R. F. L. Evans, R. W. Chantrell *et al.*, Transient ferromagnetic-like state mediating ultrafast reversal of antiferromagnetically coupled spins, *Nature* **472**, 205 (2011).
- [7] D. Steil, S. Alebrand, A. Hassdenteufel, M. Cinchetti, and M. Aeschlimann, All-optical magnetization recording by tailoring optical excitation parameters, *Phys. Rev. B* **84**, 224408 (2011).
- [8] F. Jakobs, T. Ostler, C.-H. Lambert, Y. Yang, S. Salahuddin, R. B. Wilson, J. Gorchon, J. Bokor, and U. Atxitia, Unifying femtosecond and picosecond single-pulse magnetic switching in Gd-Fe-Co, *Phys. Rev. B* **103**, 104422 (2021).
- [9] Y. Yang, R. B. Wilson, J. Gorchon, C.-H. Lambert, S. Salahuddin, and J. Bokor, Ultrafast magnetization reversal by picosecond electrical pulses, *Sci. Adv.* **3**, e1603117 (2017).
- [10] Y. Xu, M. Deb, G. Malinowski, M. Hehn, W. Zhao, and S. Mangin, Ultra-fast magnetization manipulation using single femtosecond light and hot-electrons pulse, *Adv. Mater.* **29**, 1703474 (2017).
- [11] R. B. Wilson, J. Gorchon, Y. Yang, C.-H. Lambert, S. Salahuddin, and J. Bokor, Ultrafast magnetic switching of GdFeCo with electronic heat currents, *Phys. Rev. B* **95**, 180409(R) (2017).
- [12] U. Atxitia, T. Ostler, J. Barker, R. Evans, R. Chantrell, and O. Chubykalo-Fesenko, Ultrafast dynamical path for the switching of a ferrimagnet after femtosecond heating, *Phys. Rev. B* **87**, 224417 (2013).
- [13] M. Beens, M. L. M. Lalieu, A. J. M. Deenen, R. A. Duine, and B. Koopmans, Comparing all-optical switching in synthetic-ferrimagnetic multilayers and alloys, *Phys. Rev. B* **100**, 220409(R) (2019).
- [14] V. G. Bar'yakhtar, V. I. Butrium, and B. A. Ivanov, Exchange relaxation as a mechanism of the ultrafast reorientation of spins in a two-sublattice ferrimagnet, *JETP Lett.* **98**, 289 (2013).
- [15] J. Barker, U. Atxitia, T. A. Ostler, O. Hovorka, O. Chubykalo-Fesenko, and R. W. Chantrell, Two-magnon bound state causes ultrafast thermally induced magnetisation switching, *Sci. Rep.* **3**, 3262 (2013).
- [16] A. Baral and H. C. Schneider, Magnetic switching dynamics due to ultrafast exchange scattering: A model study, *Phys. Rev. B* **91**, 100402(R) (2015).
- [17] S. Gerlach, L. Oroszlany, D. Hinzke, S. Sievering, S. Wienholdt, L. Szunyogh, and U. Nowak, Modelling ultrafast all-optical switching in synthetic ferrimagnets, *Phys. Rev. B* **95**, 224435 (2017).
- [18] V. N. Gridnev, Ferromagnetic like states and all-optical magnetization switching in ferrimagnets, *Phys. Rev. B* **98**, 014427 (2018).
- [19] A. M. Kalashnikova and V. I. Kozub, Exchange scattering as the driving force for ultrafast force for ultrafast all-optical and bias-controlled reversal in ferromagnetic metallic structures, *Phys. Rev. B* **93**, 054424 (2016).
- [20] J. H. Mentink, J. Hellsvik, D. V. Afanasiev, B. A. Ivanov, A. Kirilyuk, A. V. Kimel, O. Eriksson, M. I. Katsnelson, and T. Rasing, Ultrafast spin dynamics in multisublattice magnets, *Phys. Rev. Lett.* **108**, 057202 (2012).
- [21] A. J. Schellekens and B. Koopmans, Microscopic model for ultrafast magnetization dynamics of multisublattice magnets, *Phys. Rev. B* **87**, 020407(R) (2013).
- [22] S. Wienholdt, D. Hinzke, K. Carva, P. M. Oppeneer, and U. Nowak, Orbital-resolved spin model for thermal magnetization switching in rare-earth-based ferrimagnets, *Phys. Rev. B* **88**, 020406(R) (2013).
- [23] F. Jakobs and U. Atxitia, Universal criteria for single femtosecond pulse ultrafast magnetization switching in ferrimagnets, *Phys. Rev. Lett.* **129**, 037203 (2022).
- [24] U. Atxitia, J. Barker, R. Chantrell, and O. Chubykalo-Fesenko, Controlling the polarity of the transient ferromagnetic-like state in ferrimagnets, *Phys. Rev. B* **89**, 2244 (2014).
- [25] V. Raposo, F. Garcia-Sánchez, U. Atxitia, and E. Martinez, Realistic micromagnetic description of all-optical ultrafast switching processes in ferrimagnetic alloys, *Phys. Rev. B* **105**, 104432 (2022).
- [26] J. Pudell, A. A. Maznev, M. Herzog, M. Kronseder, C. H. Back, G. Malinowski, A. von Reppert, and M. Bargheer, Layer specific observation of slow thermal equilibration in ultrathin metallic nanostructures by femtosecond x-ray diffraction, *Nat. Commun.* **9**, 3335 (2018).

- [27] J.-L. Bello, D. Lacour, S. Migot, J. Chanbaja, S. Mangin, and M. Hehn, Impact of interfaces on magnetic properties of GdFeCo alloys, *Appl. Phys. Lett.* **121**, 212402 (2022).
- [28] S.-S. Wellershoff, J. Hohlfeld, J. Güdde, and E. Matthias, The role of electron-phonon coupling in femtosecond laser damage of metals, *Appl. Phys. A* **69**, 505 (1999).
- [29] J. Hohlfeld, S.-S. Wellershoff, J. Güdde, U. Conrad, V. Jähnke, and E. Matthias, Electron and lattice dynamics following optical excitation of metals, *Chem. Phys.* **251**, 237 (2000).
- [30] P. E. Hopkins, M. Ding, and J. Poon, Contributions of electron and phonon transport to the thermal conductivity of GdFeCo and TbFeCo amorphous rare-earth transition-metal alloys, *J. Appl. Phys.* **111**, 103533 (2012).
- [31] P. B. Corkum, F. Brunel, N. K. Sherman, and T. Srinivasan-Rao, Thermal response of metals to ultrashort-pulse laser excitation, *Phys. Rev. Lett.* **61**, 2886 (1988).
- [32] T. Ogasawana, N. Iwata, Y. Murakami, H. Okamoto, and Y. Tokura, Submicron-scale spatial feature of ultrafast photoinduced magnetization reversal in TbFeCo thin film, *Appl. Phys. Lett.* **94**, 162507 (2009).
- [33] H.-P. D. Shieh and M. H. Kryder, Magneto-optic recording materials with direct overwrite capability, *Appl. Phys. Lett.* **49**, 473 (1986).
- [34] W. Zhang, J. Hohlfeld, T. X. Huang, J. X. Lin, M. Hehn, Y. Le Guen, G. Malinowski, W. S. Zhao, and S. Mangin, Criteria to observe a single-shot all optical switching in gd-based ferrimagnetic alloys, submitted to *Adv. Mater.*